Quantized invariant tori in Andreev billiards of mixed phase space

Z. Kaufmann,[1] A. Kormányos,[2] J. Cserti,[1] and C. J. Lambert[2]
[1]*Department of Physics of Complex Systems, Eötvös University, H-1117 Budapest, Pázmány Péter sétány 1/A, Hungary*
[2]*Department of Physics, Lancaster University, Lancaster, LA1 4YB, United Kingdom*
(Received 14 February 2006; published 29 June 2006)

Comparing the results of exact quantum calculations and those obtained from the Einstein-Brillouin-Keller–like quantization scheme of Silvestrov *et al.* [Phys. Rev. Lett. **90**, 116801 (2003)] we show that the spectrum of Andreev billiards of mixed phase space can basically be decomposed into a regular and an irregular part, similarly to normal billiards. We provide a numerical confirmation of the validity of this quantization scheme for individual eigenstates and discuss its accuracy.

DOI: 10.1103/PhysRevB.73.214526 PACS number(s): 74.45.+c, 05.45.Mt, 03.65.Sq

For quantum systems, whose classical analogues have mixed dynamics, the separation of the spectra into regular and irregular parts goes back to Percival.[1] Here the term "regular" refers to such energy levels, which correspond to quantized invariant tori, while "irregular" refers to those associated with the chaotic part of the phase space. Semiclassical methods, such as Einstein-Brillouin-Keller (EBK) quantization,[2] have given a deep understanding of the influence of the classical dynamics on the quantum spectrum (see, e.g., Refs. 3–5 and references therein).

Recently a new type of quantum dot system, comprising normal-superconductor (NS) interface has attracted considerable attention. These systems are commonly called "Andreev billiards" (ABs).[6,7] The name derives from the specific scattering process taking place at the NS interface, namely, the Andreev reflection,[8] whereby an impinging electronlike quasiparticle with energy ε (measured from the Fermi energy E_F) is coherently scattered into a hole (and vice versa) if ε is smaller than the superconducting gap Δ (for details see, e.g., Ref. 7). Unlike specular reflection, this scattering process is accompanied by the (approximate) reversal of all velocity components, thereby giving rise to a peculiar classical dynamics. In a recent paper[9] we have presented evidence that in general the phase space of these systems is mixed. Thus the question naturally arises, of whether one can perform a similar separation of the spectrum into regular and irregular parts as in normal systems. While the influence of different regions of the mixed phase space of an *isolated* normal dot on the density of states of the corresponding ABs has been adressed beforehand[10] to our knowledge no study has tried to answer the above question regarding the individual energy levels and taking into account the peculiar dynamics of the *whole* NS system. Our work is aimed to be the first step towards the answer by studying a simple yet nontrivial two-dimensional (2D) example.

In our study we shall use semiclassical and quantum mechanical tools to identify the regular eigenstates. Quantum mechanically, these systems can be described by the Bogoliubov-de Gennes equations.[11] From semiclassical point of view, this implies that the EBK quantization has to be generalized to the case of spinor wave function. Such a multicomponent semiclassical theory for the NS systems has been developed in Ref. 12 and it was shown that the EBK quantization of normal systems can also be generalized to integrable NS systems. Indeed, in Ref. 13 a good agreement between semiclassical and quantum calculations has been found for an integrable AB. Another important idea regarding the quantization of NS systems was introduced in Refs. 14 and 15 for cases where for $\varepsilon > 0$ the classical dynamics is, strictly speaking, non-integrable, but there is an adiabatic invariant. At zero magnetic field the invariant is the time $T(\varepsilon)$ between subsequent Andreev reflections. According to this approach, for the purpose of semiclassical quantization, one can consider the curves of constant T at $\varepsilon = 0$.

In our work we benefit from both of the studies.[12,14] As it will be shown below, the dynamics in certain regions of the phase space is quasi-integrable. By quasi-integrable we mean regions which contain mostly tori, on which the dynamics is similar to that of integrable normal systems. Therefore we expect that for these islands of regular motion the results of Ref. 12 apply. However, the analytical calculations can be performed only in the adiabatic approximation,[14] whose accuracy will also be discussed.

The model system we used in our calculations is the Sinai-Andreev (SA) billiard.[9,16] It consists of a Sinai-billiard-shaped normal dot and an attached (infinite) superconducting lead as shown in Fig. 1(c). Classically, in the phase space of this model we have found a large stability island [see Fig. 1(a)]. Its existence can be expected, since it is centered on the shortest unstable periodic orbit of the isolated normal dot (which corresponds to the motion along the bottom wall) and the presence of the superconductor, i.e., Andreev reflection can stabilize this orbit. To prove this, we consider the dynamics on the Poincaré section (PS) which we define in the following way: we record the position y and the tangential velocity component v_y in units of $v_e = v_F\sqrt{1+\tilde{\varepsilon}}$ when the Andreev reflection results in a departing electron quasiparticle, i.e., whenever a hole impinges on the NS interface (here $\tilde{\varepsilon} = \varepsilon / E_F$, v_F is the Fermi velocity and y is measured from the lower edge of the interface). Suppose now that an electron departs from the interface and after returning to it becomes Andreev-reflected. Using simple geometrical considerations and taking into account the Andreev reflection law[17,18] one finds that for $y \ll 1$, $v_y \ll v_e$ the linearized equations of motion for the phase space coordinates $y, \tilde{v}_y = v_y / v_e$ of the quasiparticle is given by the stability matrix

$$M(\varepsilon) = \begin{pmatrix} 1 - 2d/R & 2d(1-d/R) \\ \gamma 2/R & \gamma(2d/R - 1) \end{pmatrix}, \tag{1}$$

where $\gamma = \sqrt{1+\tilde{\varepsilon}}/\sqrt{1-\tilde{\varepsilon}}$ and the geometrical parameters d, R are defined in Fig. 1(c). The motion of the emerging hole can

 ©2006 The American Physical Society

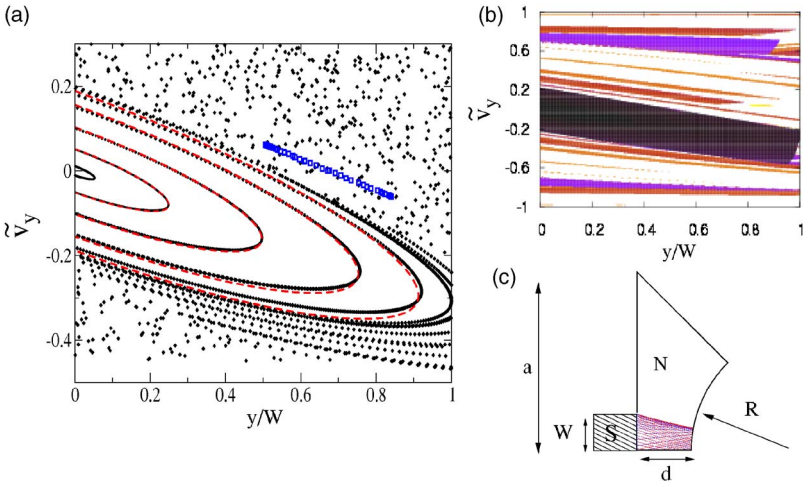

FIG. 1. (Color online) Enlargement of a part of the PS around $\tilde{v}_y=0$ (a) (for the geometrical and other parameters see Ref. 19). Each dot represents a starting point of an electron trajectory. The (red) dashed curves show the ellipse-approximation given by Eq. (2), for different T_0's. The (blue) squares denote an another, thin regular island. An alternative view of PS showing bands of approximately constant T_{eh} denoted by different colors (b). Only bands with $T_{eh}<6a/v_F$ are shown. One of the tori shown in (a) is projected onto the real space (c).

then be described by $M(-\varepsilon)$. However, by construction the Poincaré map consists only of the starting coordinates of electron trajectories, therefore the motion in the $(y,\tilde{v}_y)$ plane is given by $M_{eh}=M(-\varepsilon)M(\varepsilon)$. The periodic orbit is stable, if the trace of the matrix M_{eh} is less than 2, which gives the condition $0<d<R/(\gamma-1)$. Since $\varepsilon \ll E_F$ in our calculations, $1/(\gamma-1)\approx 1/\tilde{\varepsilon} \gg 1$ and the periodic orbit is stable for wide range of values of the parameters d and R.

Part of the PS around the stable periodic orbit is shown in Fig. 1(a). As expected, we find numerically that there are truly invariant curves around the stable periodic orbit forming an island of regular motion. This regular island, which can be clearly seen in the middle of Fig. 1(a) is surrounded by intermittent-like regions. Beyond there are chaotic seas intervowen with other intermittent regions and there is at least one another smaller regular island. As pointed out in our previous paper,[9] this structure is due to the interplay of nonexact retracing for $\tilde{\varepsilon}>0$ and the presence of the so-called "critical points" which separate the normal and the superconducting segments of the billiard boundary.

Because of its importance in the semiclassical quantization, we now focus on the energy dependence of the time $T_{eh}(y,\tilde{v}_y,\tilde{\varepsilon})$ of the electron-hole orbit between two section with the PS in the regular island. Following the electron-hole orbits which trace out the invariant curves $\mathcal{C}_{\text{inv}}$ in Fig. 1(a), we have found numerically that (a) the variation of $T_{eh}(y,\tilde{v}_y,\tilde{\varepsilon})$ corresponding to subsequent points on the invariant curves is only $O(\tilde{\varepsilon}^3)$, i.e., T_{eh} is an adiabatic invariant (b) $T_{eh}=2T(y,\tilde{v}_y,\tilde{\varepsilon}=0)+O(\tilde{\varepsilon}^2)$, where we denoted by T the time between *subsequent* Andreev-reflections for $\tilde{\varepsilon}=0$. An important consequence of the above observations is the following: if we denote by $\mathcal{C}_{T_0}$ the $T(y,\tilde{v}_y,\tilde{\varepsilon}=0)=T_0$ curves on the PS, then considering any point $(y,\tilde{v}_y)$ on $\mathcal{C}_{T_0}$, for finite $\tilde{\varepsilon}$ the invariant curve $\mathcal{C}_{\text{inv}}$ which contains this particular point will always be in $O(\varepsilon^2)$ vicinity of $\mathcal{C}_{T_0}$. This will be important later on when we discuss the semiclassical quantization of this regular island: it can be shown[12,14] that one of the action integrals to be calculated equals the area enclosed by $\mathcal{C}_{\text{inv}}$, which can be then approximated by the area enclosed by $\mathcal{C}_{T_0}$, since the difference is of higher order than $\tilde{\varepsilon} \ll 1$. A similar conclusion has been drawn in Ref. 14.

An alternative view of the PS can be obtained by denoting with different colors those regions, which correspond to approximately constant T_{eh}. These regions, which usually appear as narrow bands in Fig. 1(b) are often not easily recognizable on the PS since they do not always show ordered patterns such as those indicating the presence of intermittent-like motion around the quasi-integrable island in Fig. 1(a). [The large dark region in the middle of Fig. 1(b) corresponds to the regular island and the surrounding intermittent region in Fig. 1(a).] As we will briefly discuss later, the importance of these bands lies in the fact that some of them can be associated to certain eigenstates.

Before turning to the adiabatic quantization, we note that for a different W, and larger value of $\tilde{\varepsilon}$, in the regular island we have also found structures resembling very much the secondary island chains known from normal KAM systems. It would be an interesting future project to investigate the properties of the classical dynamics in more detail to explore the exact nature of the similarities with KAM systems. However, for the parameters[19] used in the present study, these "secondary islands," if they exist, are much smaller than Planck's constant h and thus do not play any role in our further discussion.

We now proceed with the adiabatic quantization[14] of the regular island shown in Fig 1(a). The semiclassical energies can be obtained by quantizing the action integrals $I_i=1/2\pi \oint_{\mathcal{C}_i} \mathbf{p}d\mathbf{q}$, $i=1,2$, calculated along the $\mathcal{C}_i$ irreducible closed contours on the adiabatic tori. The curve $\mathcal{C}_{T_0}$ can be chosen as the integration contour $\mathcal{C}_1$ and therefore I_1 equals the enclosed area on the PS. One can show that for $y,\tilde{v}_y \ll 1$ the curve $\mathcal{C}_{T_0}$ is semiellipse given by the following equation:

$$(L-2d)R^2 = Fy^2 + G\tilde{v}_y y + H\tilde{v}_y^2, \tag{2}$$

where $F=(2d+R)$, $G=4d(d+R)$, $H=FG/4$, and $L=v_F T_0$. Comparison of the above curve for different T_0's and the numerically calculated PS of the corresponding tori for $\tilde{\varepsilon}=0.0105$ is shown in Fig. 1(a). One can observe that the agreement is very good for the inner tori, while for those closer to the border of the regular island there is a small but noticeable deviation since the assumption $y,\tilde{v}_y \ll 1$ does not hold. Quantizing the area enclosed by $\mathcal{C}_{T_0}$ one finds the condition

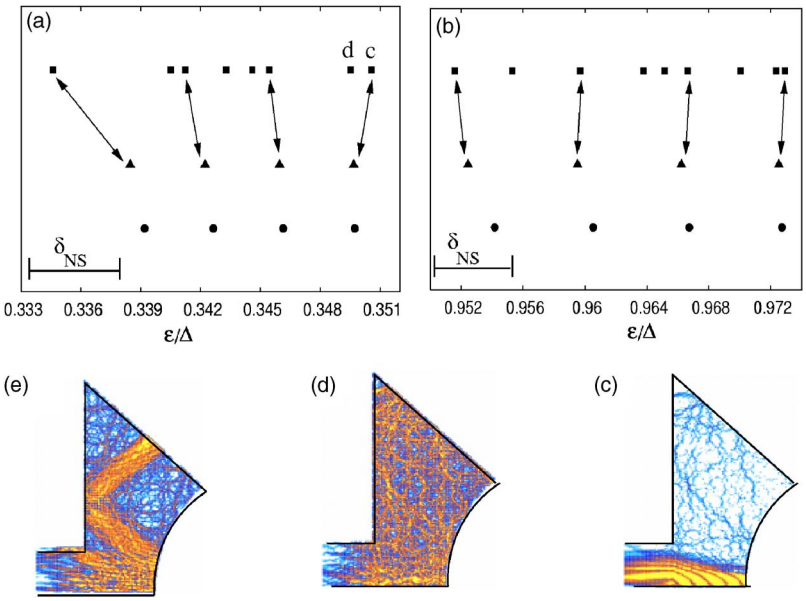

FIG. 2. (Color online) Quantum eigenenergies (squares), the results of the adiabatic quantization using Eq. (3) (circles) and by taking into account the exact shape of $\mathcal{C}_{T_0}$ (triangles) for $n=0$ (a) and $n=1$ (b). The arrows show which quantum and semiclassical energies correspond to each other. The bars show the magnitude of the mean level spacing $\delta_{\mathrm{NS}}=\delta_N/2$. The square modulus $|u(\mathbf{r})|^2$ of the electron components of the wave functions corresponding to certain eigenenergies as indicated by the letters c, d in Fig. 2(a) are seen in (c), (d). The $|u(\mathbf{r})|^2$ for the state at $\varepsilon/\Delta=0.3202$ corresponding to a band of approximately constant T_{eh} starting at $y=0$, $\tilde{v}_y=\pm 0.4$ in Fig. 1(b) is shown in (e).

$$\frac{1}{8}\frac{(L-2d)R}{\sqrt{d(d+R)}}p_F=\hbar\left(m+\frac{3}{4}\right), \tag{3}$$

where $m=0,1,2,\ldots$, and the Maslov index is 3/4 since one caustic and one hard wall is encountered along the integration contour.

The second action integral I_2 in the adiabatic approximation is to be calculated along a self-retracing electron-hole orbit. Since the particles move ballistically inside the normal dot, the quantization condition reads

$$(p_e-p_h)L=2\pi\hbar\left[n+\frac{1}{\pi}\arccos(\varepsilon/\Delta)\right]. \tag{4}$$

Here $p_e(\tilde{\varepsilon})=p_F\sqrt{1+\tilde{\varepsilon}}$ and $p_h(\tilde{\varepsilon})=p_e(-\tilde{\varepsilon})$ are the magnitudes of the electron's and hole's momentum respectively, $n=0,1,2,\ldots$, and with the $\arccos(\varepsilon/\Delta)$ term we take into account the phase shift due to the Andreev-reflection. Combining Eqs. (3) and (4) one arrives at an implicit equation for the eigenvalues ε_{nm} which can be solved numerically for each value of n and m.

Before comparing the semiclassical and exact quantum calculations, we briefly discuss the accuracy of the employed adiabatic quantization scheme in our system. There are two sources of error: the first is in the derivation of Eqs. (3) and (4) where we considered the invariant surfaces in the phase space for $\tilde{\varepsilon}=0$. However, due to the nonexact retracing, the dynamics is different for finite $\tilde{\varepsilon}$. Since in the quantum system the excitation energies $\tilde{\varepsilon}_{nm}$ are always finite, one should calculate the action integral I_1 using the invariant curves $\mathcal{C}_{\mathrm{inv}}$, whereas in case of I_2 one should take into account that for $\tilde{\varepsilon}>0$ the hole does not retrace exactly the path of the electron, and one should choose the integration contour accordingly. It turns out, however, that for the main regular island in Fig. 2(a) the results for I_1 and I_2 do not change in first order of $\tilde{\varepsilon}$ even if we take into account the effects of finite $\tilde{\varepsilon}$ on classical dynamics. Namely, as we have already pointed out, the difference between the areas enclosed by a $\mathcal{C}_{\mathrm{inv}}$ and a corresponding $\mathcal{C}_{T_0}$ is only of $O(\tilde{\varepsilon}^2)$ and therefore I_1 is accurate to first order in $\tilde{\varepsilon}$. Considering I_2, we checked the accuracy of Eq. (4) by taking as an integration contour $\mathcal{C}_2$ a nonretracing electron-hole orbit and then we closed the contour on the PS. After lengthy calculations we have found that the first correction to the result given by Eq. (4) is of the order of $\tilde{\varepsilon}^3$.

The second source of error is that in order to calculate I_1 we approximated the curves $\mathcal{C}_{T_0}$ by the semiellipses given by Eq. (2). This certainly introduces inaccuracy in case of adiabatic tori close to the border of the regular island, for which the conditions $y,\tilde{v}_y\ll 1$ do not rigorously hold. Therefore we checked our analytical results in the following way: first we numerically determined those $\mathcal{C}_{T_0}$ curves on PS for which the enclosed area is $\hbar(m+3/4)$, $m=0,1,\ldots$. Then reading off the T_0 values corresponding to these curves and using Eq. (4) we recalculated the semiclasssical energies. The results are summarized in Figs. 2(a) and 2(b) and will be discussed below.

We now compare the results of the quantum mechanical and semiclassical calculations and show that the semiclassical energies agree remarkably well with the exact quantum ones. The quantum treatment of the system is based on the Bogoliubov-de Gennes equations[11] and is briefly described in Ref. 9. It is assumed that the superconducting pair potential Δ is constant inside the lead and zero in the N region[7] and we work in the regime $\delta_N\ll E_T\ll\Delta\ll E_F$[7] where δ_N is the mean level spacing of the isolated normal dot and E_T is the Thouless energy.[19] The area of the regular island on the PS is $\approx 4\ h$ and therefore we expected eight regular eigenstates in the spectrum, corresponding to quantum numbers $n=0,1$, $m=0,1,2,3$. [For the parameters[19] used in our calculation Eqs. (3) and (4) do not have real solution for larger n, while the values of m are limited by the size of the stability island.]

Comparison of the semiclassical predictions for $n=0,1$, $m=1,\ldots,4$ and the exact quantum mechanical eigenvalues lying roughly in the same energy range can be seen in Figs. 2(a) and 2(b). This shows that there are twice as many quantum eigenenergies as semiclassical ones and at first sight it is

not obvious which of the eigenstates should be considered as regular ones. To identify the eigenstates which correspond to quantized tori we now examine the eigenfunctions. Similarly to normal billiards[20] we have found that the wave function of certain eigenstates show strong localization (both the electron and the hole components) onto classical objects (see also Refs. 9 and 13). This can be either a torus [compare Fig. 2(c) and Fig. 1(c)], or a bunch of trajectories [see, e.g., Fig. 2(e)] corresponding to a band of approximately constant T_{eh} in Fig. 1(b).

Computing, e.g., the eigenfunctions belonging to the eigenvalues shown in Fig. 2(a) reveals that only four of them are localized [as in Fig. 2(c)], three others display an apparently random interference pattern and cover the normal dot in roughly uniform way [as in Fig. 2(d)], while one of them is of intermediate nature. [The picture is very similar in case of Fig. 2(b)]. As an example, we show the electron component of those two eigenstates energies of which are very close to the $n=0$, $m=0$ semiclassical one [see Figs. 2(c) and 2(d)]. One can clearly see that one of them is chaotic, while the other is localized onto a classical torus. Thus the criteria for accepting that a quantum eigenstate corresponds to a quantized torus are the vicinity of the eigenenergy to the semiclassical prediction *and* localization of the eigenfunction. Based on these two criteria, we indeed identified 4+4 regular eigenstates (for the $n=0,1$, $m=0,\ldots,3$ cases) in the spectrum. The accuracy of the adiabatic quantization is remarkable, since using the numerically determined $\mathcal{C}_{T_0}$ for the semiclassical quantization shows that the difference between the quantum and semiclassical energies is $\sim 10^{-1}\delta_{\mathrm{NS}}$, except for the $n=0$, $m=3$ eigenstate [the leftmost one in Fig. 2(a)], for which it is $0.83\delta_{\mathrm{NS}}$ (here $\delta_{\mathrm{NS}}=\delta_N/2$ is the mean level spacing of the NS system). If one approximates the curves $\mathcal{C}_{T_0}$ by semiellipses as in Eq. (3), the agreement remains the same for the states with quantum number $m=0,1$ and slightly deteriorates for the $m=2,3$ states. Finally, the observation that chaotic eigenstates are intermixed with regular ones in the given energy interval suggests that the Berry-Robnik conjecture[21] for the spectrum of (normal) systems with mixed classical dynamics might also hold for ABs.

In addition to the regular eigenstates discussed so far, we have found that some of the bands of nearly constant T_{eh} shown in Fig. 1(b) with intermittent dynamics also support one or more quantum eigenstates. The energies of these eigenstates can also be obtained with semiclassical methods, although not as accurately as in the previous case. We found that calculating the average time $\bar{T}_{eh}$ of an electron-hole orbit in a given band and then using Eq. (4) with $\bar{L}=v_F\bar{T}_{eh}$ one can usually predict the quantum eigenvalues with an error $\lesssim\delta_{\mathrm{NS}}$. As an example, for the eigenstate shown in Fig. 2(e) the quantum calculation gives $\varepsilon/\Delta=0.3202$ while for $n=1$ the semiclassical result is 0.3239, giving an error of $0.8\delta_{\mathrm{NS}}$. [There is also a quantum state which corresponds to the $n=0$ semiclassical one, but it is not as clearly localized as the one shown in Fig. 2(e).]

In summary, semiclassical analysis and the wave function computation enable the classification of certain eigenstates as regular ones for Andreev billiards of mixed phase space. For regular states we present the first numerical calculation to show that EBK-like quantization scheme yields good agreement with the quantum results. Moreover, other states are either chaotic or can be associated with bands on the PS for which the time until the next Poincaré section is approximately constant.

We would like to thank H. Schomerus for useful discussions. This work is supported by E. C. Contract No. MRTN-CT-2003-504574, EPSRC, the Hungarian-British TeT.

[1] I. C. Percival, J. Phys. B **6**, L229 (1973).
[2] M. Brack and R. K. Bhaduri, *Semiclassical Physics* (Addison-Wesley, New York, 1997); M. C. Gutzwiller, *Chaos in Classical and Quantum Mechanics* (Springer-Verlag, New York, 1990).
[3] M. V. Berry, in *Les Houches Lecture Series Session XXXVI* (North Holland, Amsterdam, 1983), pp. 171–271.
[4] O. Bohigas, S. Tomsovic, and D. Ullmo, Phys. Rep. **223**, 43 (1993).
[5] R. Ketzmerick, L. Hufnagel, F. Steinbach, and M. Weiss, Phys. Rev. Lett. **85**, 1214 (2000).
[6] I. Kosztin, D. L. Maslov, and P. M. Goldbart, Phys. Rev. Lett. **75**, 1735 (1995).
[7] C. W. J. Beenakker, Lect. Notes Phys. **667**, 131 (2005).
[8] A. F. Andreev, Zh. Eksp. Teor. Fiz. **46**, 1823 (1964) [Sov. Phys. JETP **19**, 1228 (1964)].
[9] A. Kormányos, Z. Kaufmann, J. Cserti, and C. J. Lambert, Phys. Rev. Lett. **96**, 237002 (2006).
[10] H. Schomerus and C. W. J. Beenakker, Phys. Rev. Lett. **82**, 2951 (1999).
[11] P. G. de Gennes, *Superconductivity of Metals and Alloys* (Benjamin, New York, 1996).
[12] K. P. Duncan and B. L. Györffy, Ann. Phys. (N.Y.) **298**, 273 (2002).
[13] F. Libisch, S. Rotter, and J. Burgdörfer, Phys. Rev. B **73**, 045324 (2006).
[14] P. G. Silvestrov, M. C. Goorden, and C. W. J. Beenakker, Phys. Rev. Lett. **90**, 116801 (2003).
[15] M. C. Goorden, Ph. Jacquod, and C. W. J. Beenakker, Phys. Rev. B **72**, 064526 (2005).
[16] A. Kormányos, Z. Kaufmann, C. J. Lambert, and J. Cserti, Phys. Rev. B **70**, 052512 (2004).
[17] A. V. Shytov, P. A. Lee, and L. S. Levitov, Usp. Fiz. Nauk **168**, 222 (1998) [Phys. Usp. **41**, 207 (1998)].
[18] I. Adagideli and P. M. Goldbart, Int. J. Mod. Phys. B **16**, 1381 (2002).
[19] Throughout this paper the number of open channels in the lead is the integer part of $k_F W/\pi=25.51$ (k_F is the Fermi wave number), while $\Delta_0/E_F=0.03$ and $W=0.21$, $R=0.7$ in units of a. For Fig. 1(a) we used $\tilde{\varepsilon}=0.0105$ in the actual calculation.
[20] G. Veble, M. Robnik, and J. Liu, J. Phys. A **32**, 6423 (1999).
[21] M. V. Berry and M. Robnik, J. Phys. A **17**, 2413 (1984).